Oncogene (2013) 32, 872–882

www.nature.com/onc

Open

ORIGINAL ARTICLE

Mer receptor tyrosine kinase promotes invasion and survival in glioblastoma multiforme

Y Wang[1], G Moncayo[1], P Morin Jr[1,5], G Xue[1], M Grzmil[1], MM Lino[2], V Clément-Schatlo[3], S Frank[4], A Merlo[2,6] and BA Hemmings[1]

The infiltration of glioma cells into adjacent tissue is one of the major obstacles in the therapeutic management of malignant brain tumours, in most cases precluding complete surgical resection. Consequently, malignant glioma patients almost invariably experience tumour recurrences. Within the brain, glioma cells migrate rapidly either amoeboidly or mesenchymally to invade surrounding structures, in dependence on the extracellular environment. In addition, radiotherapy, frequently applied as adjuvant therapeutic modality, may enhance tumour cell mobility. Here, we show that the receptor tyrosine kinase Mer (MerTK) is overexpressed in glioblastoma multiforme (GBM) and that this is accompanied with increased invasive potential. MerTK expression is maintained in primary GBM-derived tumour spheres under stem cell culture conditions but diminishes significantly in serum-containing cultures with concomitant downregulation of Nestin and Sox2. Depletion of MerTK disrupts the rounded morphology of glioma cells and decreases their invasive capacity. Furthermore, the expression and phosphorylation of myosin light chain 2 are strongly associated with MerTK activity, indicating that the effect of MerTK on glioma cell invasion is mediated by actomyosin contractility. Finally, DNA damage robustly triggers the upregulation and phosphorylation of MerTK, which protects cells from apoptosis. This effect is strongly impaired upon MerTK depletion or overexpression of an inactive MerTK mutant. Collectively, our data suggests that MerTK is a novel therapeutic target in the treatment of the malignant gliomas.

Oncogene (2013) **32,** 872–882; doi:10.1038/onc.2012.104; published online 2 April 2012

Keywords: glioblastoma multiforme (GBM); MerTK; invasiveness; apoptosis; actomyosin contractility

INTRODUCTION

Glioblastoma multiforme (GBM) is the most common malignant brain tumour in adults, characterized by rapid growth, high degree of invasiveness and resistance to standard adjuvant treatments. GBMs have been subdivided into 'primary' and 'secondary' on the basis of molecular signatures and clinical characteristics. Secondary GBMs derive from the progressive transformation from a preexisting lower grade gliomas, whereas primary GBMs have no evidence of prior symptoms or antecedent lower grade glial neoplasias.[1] Although the median survival after diagnosis of GBM patients has improved from 10 to 14 months in the last decade, there is still no effective treatment for this malignant cancer.[2] Thus, the demand remains for therapies improving survival and maintaining quality of life.

The infiltrative growth behaviour of GBM is a major therapeutic challenge. Clinical treatments that include radio/chemotherapy after surgery enrich $CD133^+$ cells and increase tumour aggressiveness.[3,4] The neural extracellular matrix lacks typical proteins of other tissues, such as collagen, fibronectin and type-I laminin, and instead consists of hyaluronic acid and associated glycoproteins as well as proteoglycan fibres.[5] Migrating glioma cells *in vivo* have a rounded, amoeboid morphology and invade adjacent brain tissue by gliding through the limited extracellular space.[6] In addition, coordinated crossbridging between non-muscle myosin II and actin is shown to be crucial for glioma cell invasion *in vivo*.[6]

Tyrosine kinase Mer (MerTK), which is named after its predominant expression in monocytes, cells of epithelial and reproductive origin,[7] belongs to the Tyro3, Axl and Mer receptor tyrosine kinase family. The ligands of Tyro3, Axl and Mer receptors are protein S and growth arrest-specific gene 6 (Gas6).[8] As MerTK has a low-binding affinity for these ligands, other unknown ligand(s) or conditions may be required for MerTK activation.[9] Full activation of MerTK requires the autophosphorylation of tyrosine residues 749, 753 and 754 within the kinase domain.[10] MerTK knockout mice are fertile and viable but gradually develop lupus-like autoimmune disease as well as retinal dystrophy because of reduced efficiency of apoptotic cell clearance.[11,12] Dysregulated MerTK has important roles in tumourigenesis.[13] A chimeric receptor with a substitution of the MerTK extracellular domain by macrophage colony-stimulating factor receptor is able to transform NIH3T3 cells.[14] MerTK is overexpressed in several cancer types, including mantle cell lymphomas,[15] prostate cancer,[16] breast cancer[17] and melanoma.[18] In addition, MerTK knock-in mice with ectopic expression in thymocytes and lymphocytes develop T-cell lymphoblastic leukaemia/lymphoma.[19] Recently, MerTK was found to be upregulated in the mesenchymal subtype of primary GBMs.[20] Nevertheless, the mechanisms of MerTK activation and its activity in the brain tumour progression remains unclear.

We have found that MerTK is overexpressed in GBM and GBM-derived spheres compared with non-neoplastic brain tissue

[1]Mechanisms of Cancer, Friedrich Miescher Institute for Biomedical Research, Basel, Switzerland; [2]Department of Research and Surgery, Laboratory of Molecular Neuro-oncology, University of Basel, Basel, Switzerland; [3]Department of Clinical Neurosciences, Division of Neurosurgery, Geneva University Hospitals and University of Geneva, Geneva, Switzerland and [4]Department of Neuropathology, Institute of Pathology, University of Basel, Basel, Switzerland. [5]Current address: Université de Moncton, Moncton, Canada. [6]Current address: Buchserstrasse 20, CH-3006, Bern, Switzerland. Correspondence: Dr BA Hemmings, Mechanisms of Cancer, Friedrich Miescher Institute for Biomedical Research, Maulbeerstrasse 66, Basel CH 4058, Switzerland. E-mail: brian.hemmings@fmi.ch
Received 31 August 2011; revised 17 January 2012; accepted 3 February 2012; published online 2 April 2012

and normal human astrocytes, and is mitigated upon differentiation. MerTK maintains the rounded morphology of GBM cells under stem cell culture conditions. Knockdown of MerTK decreases cell infiltrative capacity and increases cell sensitivity to etoposide-induced apoptosis. We further show that MerTK autophosphorylation is essential for its antiapoptotic and pro-invasive activities. Depletion of MerTK attenuates the expression and phosphorylation of myosin light chain 2 (P-MLC2). These results identify novel activities of MerTK in glioma cell invasion and survival.

RESULTS

MerTK is overexpressed in malignant gliomas

In previous study, we analysed 30 glioma samples by microarray analysis.[21] Consequent bioinformatics analysis identified MerTK as one of the candidate genes significantly upregulated in GBMs compared with non-neoplastic brain tissue and normal human astrocytes (data not shown). Elevated expression of MerTK in GBM samples was further validated by quantitative reverse transcriptase–PCR and western blotting (Figures 1a and b). The variation in molecular weight observed was because of differential

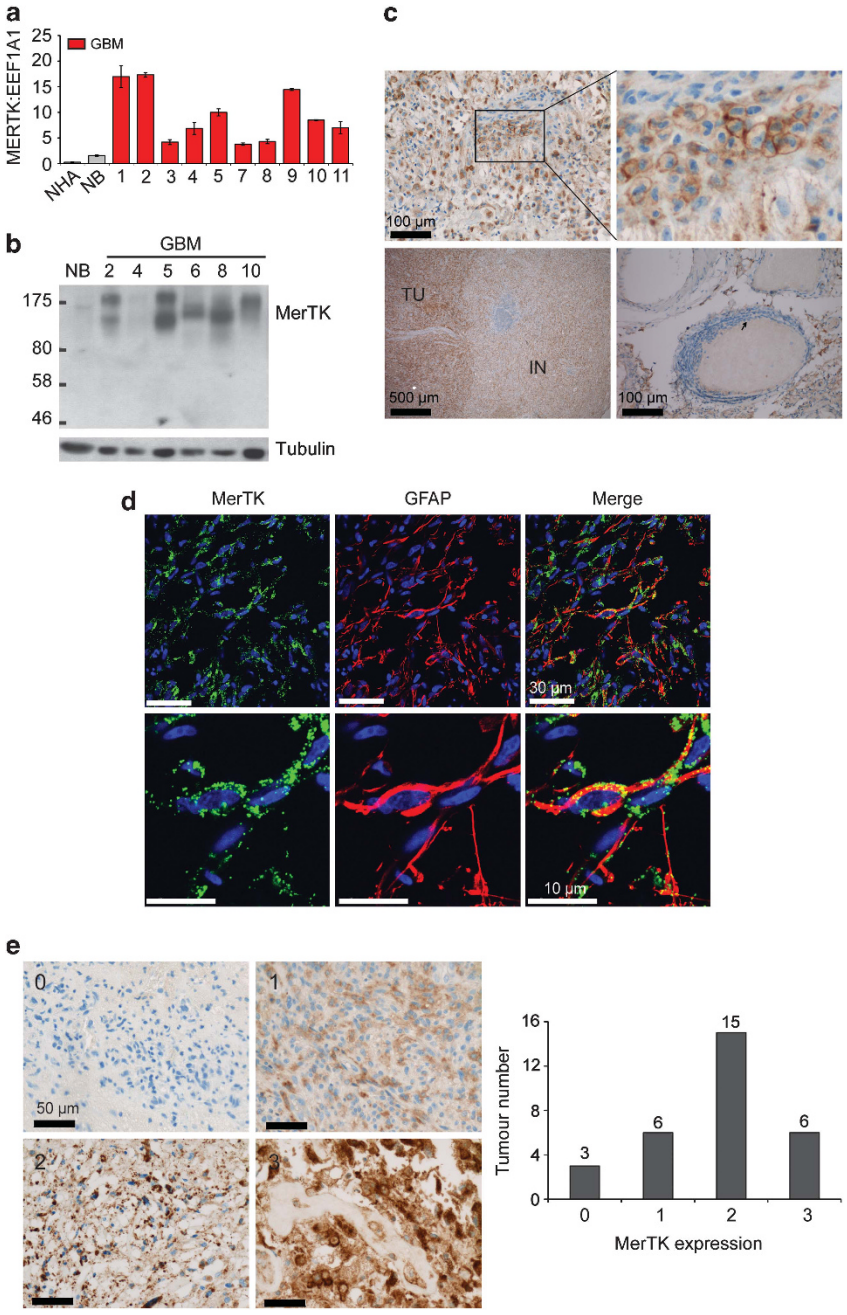

Figure 1. MerTK is overexpressed in malignant gliomas. (**a**) The endogenous MerTK mRNA level was normalized to eukaryotic translation elongation factor 1 alpha 1 expression on total RNA isolated from 10 GBM samples, 1 sample of non-neoplastic brain tissue (*NB*) and normal human astrocytes (*NHA*). (**b**) Western blotting of MerTK expression in human GBM and non-neoplastic brain tissue (*NB*). (**c**) Immunohistochemical analysis of MerTK expression in GBM samples. IN: infiltrating zone; TU: tumour mass. (**d**) Immunofluorescent staining of MerTK and GFAP in primary GBM samples. (**e**) Immunohistological scoring of MerTK expression in 30 primary GBM samples: '0' no, '1' low, '2' medium and '3' high.

glycosylation on the extracellular domain of MerTK, as confirmed by treatment of whole U937 cell lysates with the deglycosylation enzyme PNGase F, which significantly decreased the molecular weight of MerTK (Supplementary Figure 2).[7,22] To further analyse MerTK expression histologically, we generated MerTK antibodies and confirmed their specificities through western blot, immunoprecipitation (IP) and immunohistochemistry (Supplementary Figure 1). Immunohistochemical staining of human GBM samples showed that MerTK localized predominantly to the cell membrane (Figure 1c, upper images) and was expressed by cells within the solid tumour mass as well as in the infiltration zone (Figure 1c, lower left), but not in endothelial cells (Figure 1c, lower right, solid arrow). Fluorescence coimmunostaining demonstrated that MerTK was expressed by $GFAP^+$ cells of the astrocytic lineage (Figure 1d). MerTK expression was further scored in 30 primary GBM samples and found to be overexpressed in 90% of analysed tumours (27/30) (Figure 1e).

MerTK is highly expressed in GBM-derived spheres

Because of the failure of established GBM cell lines to accurately model the human disease, long-term expansion of neurospheres from primary GBMs in serum-free medium was used to more precisely reflect tumour phenotypes.[23] We analysed the expression levels of MerTK and neural stem cell markers Sox2 and Nestin in immortalized GBM cell lines cultured in serum-containing medium and in GBM spheres growing in NeuralBasal medium (NBM). Remarkably, in contrast to GBM cell lines, MerTK was highly expressed in all three GBM sphere cultures (Figure 2a), distributed specifically to the cell membrane (Figure 2b). Compared with other GBM cell lines, U373 cells had a relatively high level of endogenous MerTK (Supplementary Figure 3), Sox2 and Nestin (Figure 2a). GBM spheres GBM-7S, GBM-21S and GBM-22S growing under differentiation culture conditions showed stellate cell morphology (Figure 2c) and loss of Nestin, Sox2 and MerTK expression (Figure 2d). This discrepancy between MerTK expression in GBM spheres and immortalized GBM cell lines implies that MerTK is expressed under conditions that more precisely mimic the *in vivo* tumour microenvironment.

Knockdown of MerTK disrupts the morphology of GBM spheres

Unlike GBM-21S and GBM-22S, GBM-7S spheres showed both adherent and suspended phenotypes during maintenance

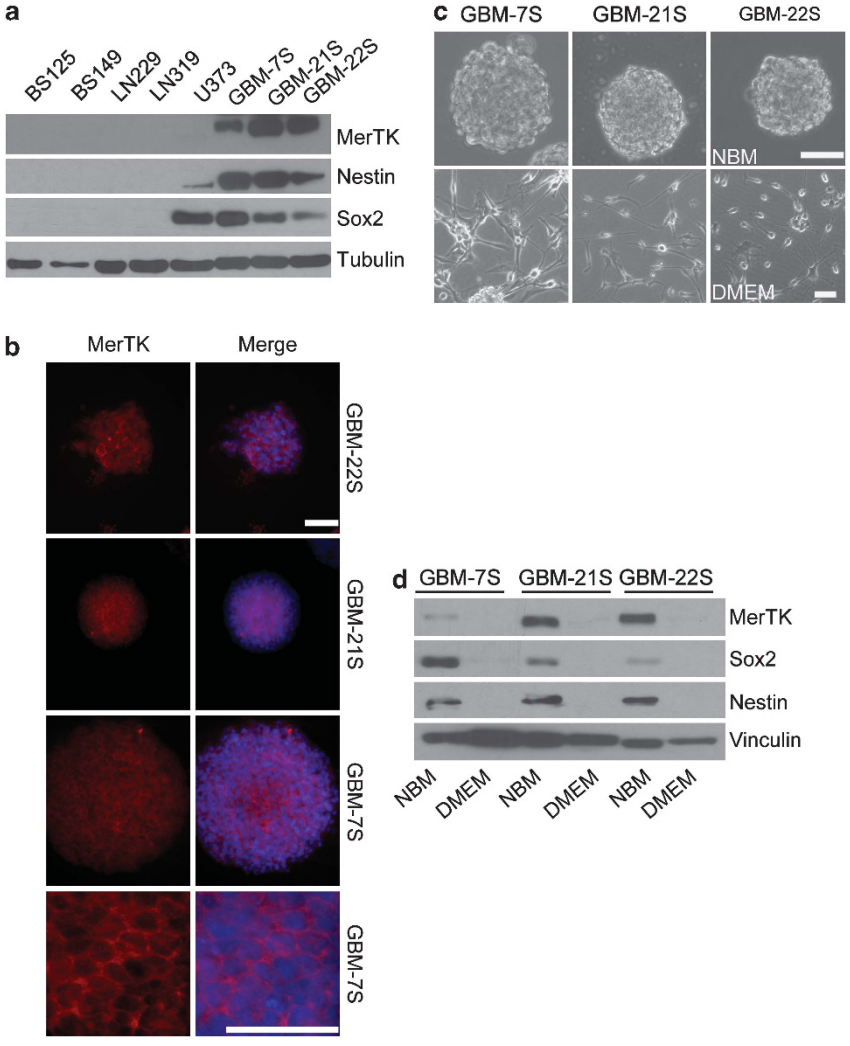

Figure 2. MerTK is highly expressed in GBM-derived spheres. (**a**) Western blotting of MerTK, Nestin and Sox2 expression in immortalized GBM cell lines and GBM-derived spheres. (**b**) Immunofluorescent staining of MerTK expression in three GBM-derived spheres. Nuclei were counterstained by 4′-6-diamidino-2-phenylindole. Scale bar 50 μm. (**c**) Morphology of three GBM-derived spheres cultured in NBM or Dulbecco's modified Eagle medium (DMEM) + 10% foetal bovine serum (FBS) for 10 days. Scale bar 50 μm. (**d**) Western blotting of MerTK, Nestin and Sox2 expression in three GBM-derived spheres cultured in NBM or in DMEM + 10% FBS for 10 days.

(Figure 3a). The differences between adherent and suspended spheres have been studied both *in vitro* and *in vivo*.[24] To examine MerTK expression in this situation, we sorted suspended spheres into fresh cultures. As shown in Figure 3a, although attachment to the substrates did not affect expression of Nestin and Sox2, MerTK was significantly downregulated. Depletion of MerTK led to cell attachment (Figures 3b and c), impaired the spherical form of GBM-7S spheres in NBM as revealed by F-actin staining (Figure 3d) and increased branchy cell cluster formation in Matrigel in the presence of NBM (Figure 3e). In fact, over 90% of cell clusters showed a spiky phenotype upon depletion of MerTK (Figure 3f). This suggests that MerTK is involved in regulation of cytoskeletal dynamics.

Active MerTK maintains rounded cell morphology and invasive capacity

U373 cells were grown under stem cell culture conditions as reported previously.[25] In these conditions, cells adopted a round morphology and formed spheres after several days (data not shown), in parallel to increased MerTK expression (Figure 4a). Interestingly, other GBM cell lines growing under stem cell culture conditions either died (data not shown) or showed adherent features with an elongated morphology (Supplementary Figure 4a). To investigate whether upregulation of MerTK is induced by the supplementation of epidermal growth factor (EGF) and basic fibroblast growth factor (bFGF) in NBM, we withdrew both growth factors and monitored MerTK expression over 5 days. Our results suggested that deprivation of these factors did not significantly affect MerTK induction (data not shown), indicating the increase of MerTK in NBM may result from autocrine effects or other nutrients in the culture medium.

In order to gain insights into the biological significance of MerTK upregulation, we depleted endogenous MerTK in U373 cells by RNA interference. Knockdown of MerTK not only induced a distinct morphological change from rounded to elongated, and subsequently in a more compact and organized sphere formation in NBM (Figure 4b, Supplementary Figure 4b), but also increased

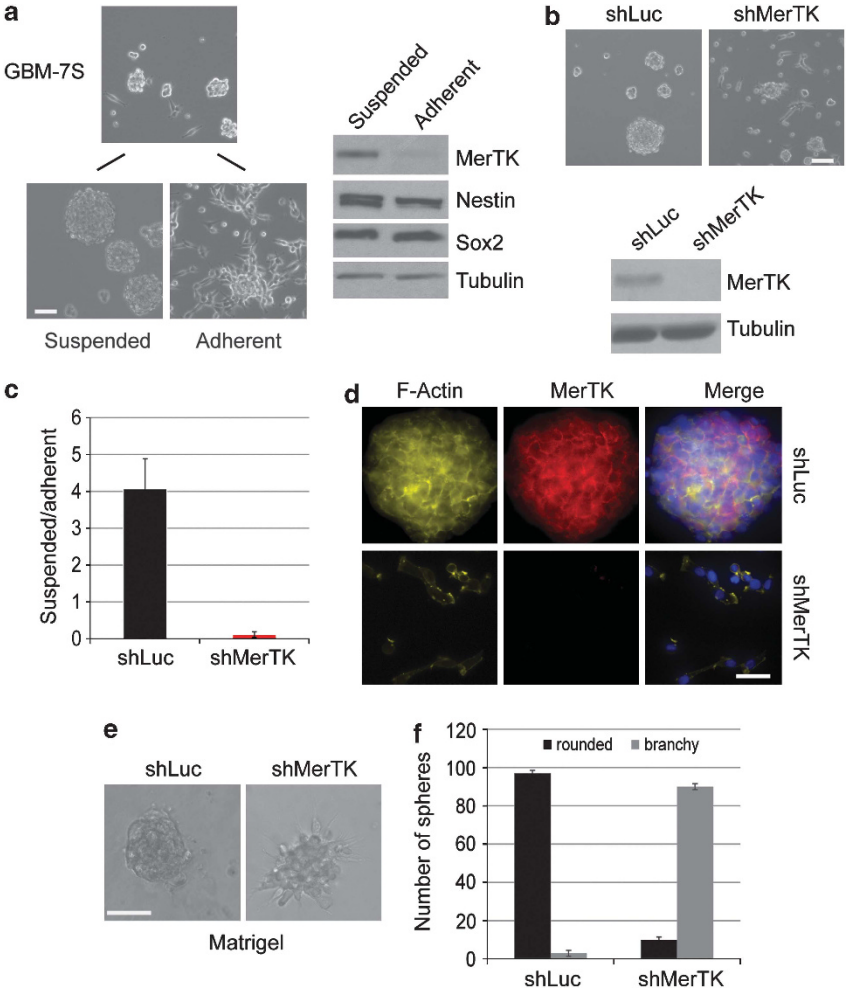

Figure 3. Knockdown of MerTK disrupts the spherical morphology of GBM spheres. (**a**) GBM-7S spheres maintained in NBM show both adherent and suspended phenotypes. Sorted adherent and suspended GBM-7S spheres were cultured in NBM for 1 week and cell lysates subjected to western blotting for Sox2, Nestin and MerTK. Scale bar 50 μm. (**b**) Phase contrast images of GBM-7S spheres expressing shLuc or shMerTK. Western blotting showed MerTK knockdown efficiency in GBM-7S spheres. Scale bar 50 μm. (**c**) Detachment assay of GBM-7S spheres expressing shLuc or shMerTK. Data are shown as the ratio of suspended to adherent cells after being dissociated and seeded in NBM for 2 h. Data are representative of experiments in triplicate and are shown as means ± s.d. (**d**) GBM-7S spheres expressing shLuc or shMerTK were stained for MerTK and F-actin. Nuclei were counterstained by 4′-6-diamidino-2-phenylindole. Scale bar 20 μm. (**e**) GBM-7S spheres expressing shLuc or shMerTK were cultured in Matrigel in the presence of NBM. Scale bar 50 μm. (**f**) Morphology quantification of GBM-7S spheres expressing shLuc or shMerTK cultured in Matrigel in the presence of NBM. Results are shown as means ± s.d. of 100 spheres from three independent experiments.

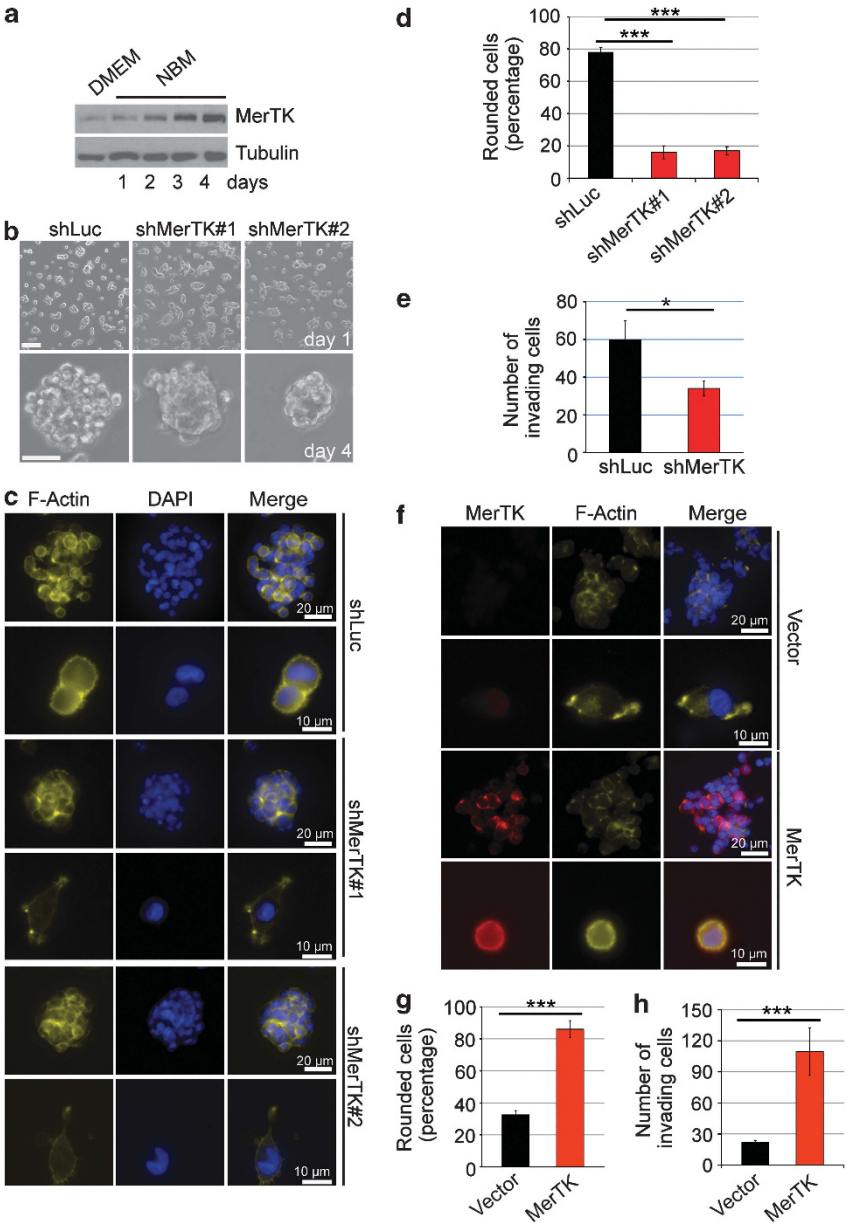

Figure 4. MerTK maintains rounded cell morphology and invasive potential. (**a**) U373 cells were grown in serum-containing (Dulbecco's modified Eagle medium) DMEM or NBM for 4 days. Cells were harvested and lysed at indicated time points for analysis of MerTK expression by western blotting. (**b**) MerTK was knocked down in U373 cells by shRNA (two different clones are shown as #1 and #2). U373shLuc and U373shMerTK#1 and #2 cells were cultured in NBM and cell morphology photographed after 1 day and 4 days. Scale bar 50 μm. (**c**) U373shLuc and U373shMerTK#1 and #2 cells were cultured in NBM for 3 days and stained for F-actin. Nuclei were counterstained by 4′-6-diamidino-2-phenylindole (DAPI). (**d**) Quantification of rounded cells stained by F-actin shown in **c**. Results are means ± s.d. of 150 cells from three independent experiments. (**e**) Analysis of the invasive potential of U373shLuc and U373shMerTK (50% of U373shMerTK#1 and 50% of U373shMerTK#2) cells. Cells were seeded in Boyden chambers for 22 h and the cells invading the membrane revealed by DAPI staining and counted under the microscope. Data are representative of experiments in triplicate and are shown as means ± s.d. The differences between U373shLuc and U373shMerTK cells are statistically significant (*$P = 0.03$). (**f**) U373shMerTK#1 cells expressing empty vector or rescue MerTK cDNA were cultured in NBM for 3 days and stained for MerTK and F-actin. Nuclei were counterstained by DAPI. (**g**) Quantification of rounded cells stained by F-actin shown in **f**. Results are means ± s.d. of 150 cells from three independent experiments. The differences are statistically significant (***$P < 0.0001$). (**h**) Analysis of the invasive potential of U373shMerTK#1 cells stably expressing empty vector or rescue MerTK cDNA. Cells were seeded in Boyden chambers for 22 h and the cells invading the membrane revealed by DAPI staining and counted under the microscope. Data are representative of experiments in triplicate and are shown as means ± s.d. The differences are statistically significant (***$P < 0.0001$).

cell attachment (Supplementary Figure 4c). Cells expressing shMerTK had a spindle mesenchymal morphology, whereas cells expressing shLuc were rounded and amoeboid in shape in Matrigel in the presence of NBM (Supplementary Figure 4d). Interestingly, cells lacking MerTK exhibited multiple membrane protrusions, whereas cells expressing shLuc displayed marked cortical F-actin staining and extensive membrane blebbings (Figure 4c); ~80% of cells lost their rounded morphology upon MerTK depletion (Figure 4d). To test whether knockdown of MerTK impairs cell infiltrative potential, we measured the invasive

capacity of U373 cells in the presence and absence of MerTK expression. As shown in Figure 4e, MerTK depletion strongly suppressed U373 cell invasion through the Matrigel. However, knockdown of MerTK did not affect U373 cell migration in these settings (data not shown).

To further demonstrate the necessity of MerTK for the maintenance of rounded cell morphology and infiltrative capacity, we reintroduced rescue cDNA expressing wild-type MerTK (MerTK-wt) into U373shMerTK#1 cells. Re-expression of MerTK significantly restored rounded cell morphology with blebbings on the cell membrane (Figures 4f and g, Supplementary Figure 4e), as well as invasive potential (Figure 4h).

In order to investigate further whether MerTK activity helps maintain rounded morphology, U373 cells stably expressing empty vector, wild-type MerTK (MerTK-wt) or MerTK mutant (MerTK-mut, Y749FY753FY754F) were cultured in NBM. Strikingly, MerTK-wt was rapidly phosphorylated and cells displayed a spherical morphology after 4 days in NBM. In contrast, cells expressing MerTK-mut were elongated and showed higher adherence, similar to MerTK-depleted U373 cells (Figures 5a and b). In fact, MerTK-mut expression was associated with changes in cellular cytoskeletal organization and resulted in compact sphere structures (Figure 5c). However, when MerTK-wt was expressed and phosphorylated, more cells became rounded in shape with extensive blebbings and showed cortical F-actin localization (Figures 5c and d). In contrast to cells expressing empty vector or MerTK-mut, MerTK-wt-expressing U373 cells possessed an enhanced invasive potential, implying an important role for MerTK phosphorylation in cell infiltration (Figure 5e).

MerTK promotes GBM cell invasion by regulating actomyosin contractility

Glioma cells migrate as mesenchymal cells in 2D but invade as neural progenitor cells in an amoeboid mode *in vivo*.[6] Without

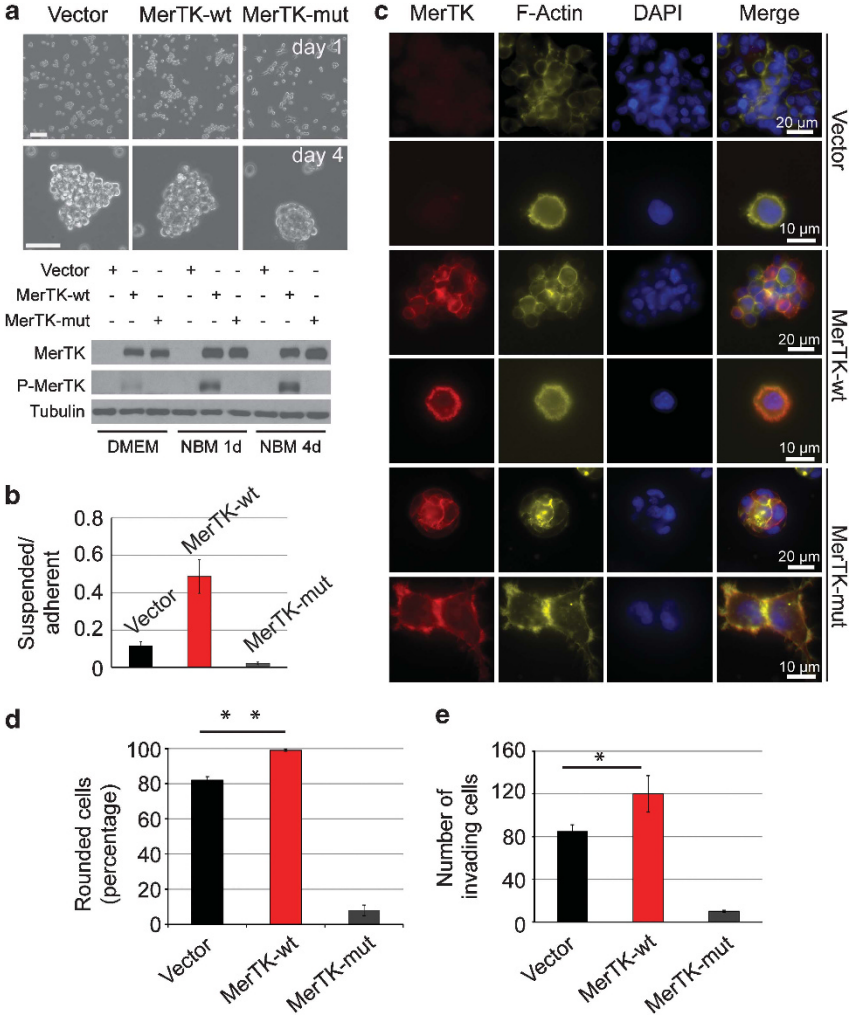

Figure 5. Autophosphorylation of MerTK is required for maintenance of rounded morphology and cell invasive capacity. (**a**) U373 cells stably expressing empty vector, MerTK-wt or MerTK-mut were cultured in NBM and cell morphology photographed after 1 and 4 days. P-MerTK and total MerTK were assayed by western blotting. Scale bar 50 μm. (**b**) Detachment assay of U373 cells expressing empty vector, MerTK-wt or MerTK-mut. Data are shown as the ratio of suspended and adherent cells after being dissociated and cultured in NBM for 48 h. Data are representative of experiments in triplicate and are shown as means ± s.d. (**c**) Immunofluorescent staining of F-actin and MerTK in U373 cells expressing empty vector, MerTK-wt or MerTK-mut and cultured in NBM for 24 h. Nuclei were counterstained by 4′-6-diamidino-2-phenylindole (DAPI). (**d**) Quantification of rounded cells revealed by F-actin staining. Results are means ± s.d. of 150 cells from three independent experiments (**$P = 0.004$). (**e**) The invasive potential of U373 cells expressing empty vector, MerTK-wt or MerTK-mut was analysed by Boyden chamber assay. The cells were seeded in the upper chamber for 22 h and invading cells stained with DAPI and counted under the microscope. Data are representative of experiments in triplicate and are shown as means ± s.d. The differences between empty vector- and MerTK-wt-expressing cells are statistically significant (*$P = 0.018$).

degrading extracellular matrix, changes in glioma cell shape allow passage of cells through gaps in the tissue environment driven by cortical actomyosin contractility.[6] Although several proteins, including kinases, have been shown to be involved in crossbridging between actin and myosin, phosphorylation at serine 19 of MLC2 is a prerequisite for actomyosin ATPase activity.[26] Morphological differences in 3D culture are commonly used to distinguish mesenchymally or amoeboidly migrating cells. As MerTK-depleted cells displayed an elongated mesenchymal phenotype, we analysed MLC2 expression and phosphorylation in U373 cells and GBM-7S spheres. Knockdown of MerTK or overexpression of MerTK-mut significantly decreased MLC2 expression and phosphorylation (Figures 6a–c). Treating U373 stable cell lines with blebbistatin, a cell-permeable molecule that specifically inhibits myosin II heavy chain ATPase activity,[27] significantly disrupted rounded cell morphology (Supplementary Figure 5a), which was attenuated upon expression of MerTK-wt (Figure 6d, Supplementary Figure 5b). This suggests that myosin II activity-controlled cell motility is dependent on active MerTK.

MerTK is induced upon DNA damage and promotes cell survival

It has been shown that inhibition of MerTK and Axl in astrocytoma cells increased chemosensitivity under differentiation culture condition.[28] In this present study, we observed that etoposide treatment substantially induced MerTK expression in adherent GBM-7S cells and led to cell detachment (Figure 7a). Knockdown of MerTK sensitized GBM-7S cells to etoposide-induced apoptosis (Figure 7b). Consistently, elevated MerTK expression was detected in U373 cells after DNA damage (Figure 7c). To further investigate the activity of MerTK in GBM, U373 cells stably expressing empty vector, MerTK-wt or MerTK-mut were treated with γ-irradiation or etoposide. Interestingly, MerTK phosphorylation was significantly increased and protected cells from apoptosis, as shown by diminished cleaved-PARP and cleaved-caspase 3 levels (Figure 7d, Supplementary Figure 6).

An early event initiating DNA damage-induced apoptosis is loss of mitochondrial membrane potential, $\Delta\psi$m.[29] Assessing the apoptotic fraction of cells by measuring $\Delta\psi$m after etoposide treatment, we recorded increases in this fraction from 4.5% to 59.3% and from 5.1% to 56.9% in empty vector- and MerTK-mut-expressing U373

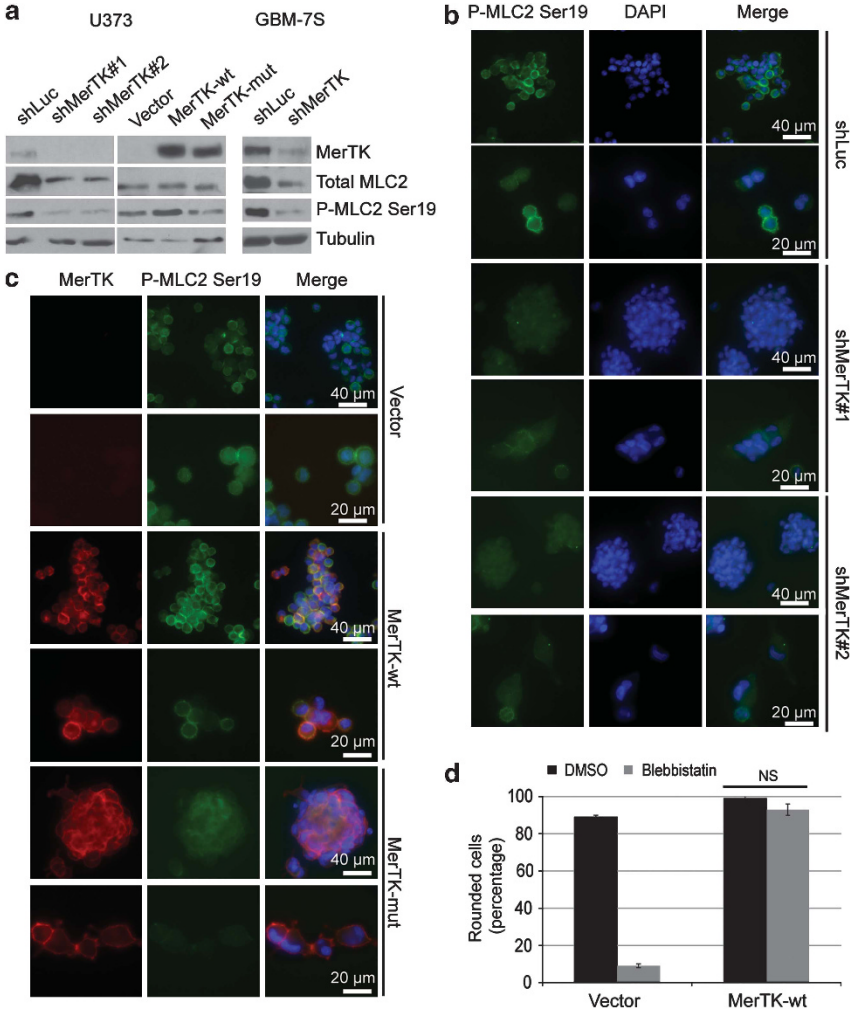

Figure 6. MerTK promotes GBM cell invasion by regulating actomyosin contractility. (**a**) Western blotting of total MerTK, total MLC2 and P-MLC2 Ser19 in U373 and GBM-7S stable cell lines. U373shLuc, U373shMerTK#1 and #2 cells were cultured in NBM for 3 days. U373 cells stably expressing empty vector, MerTK-wt or MerTK-mut were cultured in NBM for 24 h. (**b**) Immunofluorescent staining of P-MLC2 Ser19 in U373shLuc, U373shMerTK#1 and #2 cells cultured in NBM for 3 days. Nuclei were counterstained by 4′-6-diamidino-2-phenylindole (DAPI). (**c**) Immunofluorescent staining of P-MLC2 Ser19 and MerTK in U373 cells expressing empty vector, MerTK-wt or MerTK-mut cultured in NBM for 24 h. Nuclei were counterstained by DAPI. (**d**) Quantification of rounded cells stained by F-actin. U373 cells expressing empty vector or MerTK-wt seeded in NBM and treated with 10 μM blebbistatin (Sigma) for 90 min. Results are means ± s.d. of 150 cells from three independent experiments.

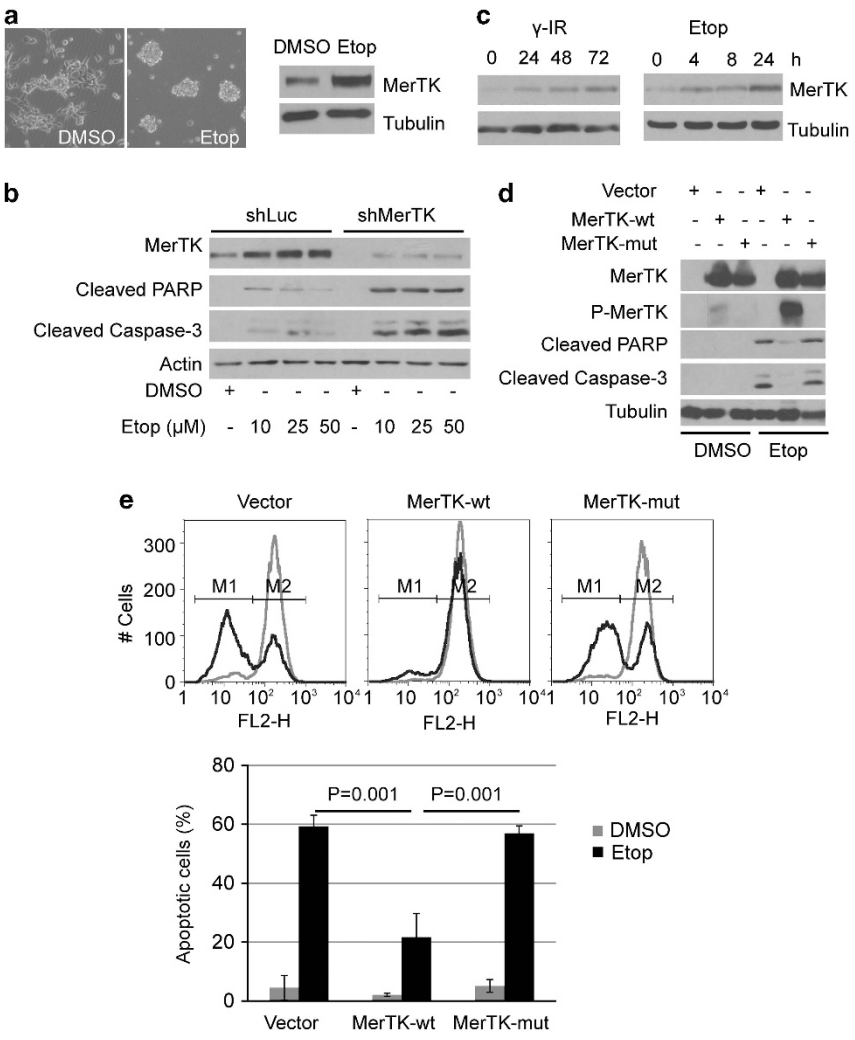

Figure 7. MerTK is induced upon DNA damage and promotes cell survival. (**a**) Adherent GBM-7S cells were treated with 50 μM etoposide (Etop, Sigma) for 48 h and expression of MerTK analysed by western blotting. Scale bar 50 μm. (**b**) Western blotting for cleaved PARP and cleaved caspase-3 in MerTK-knockdown or shLuc-expressing GBM-7S spheres treated with etoposide at different doses for 40 h. DMSO was used as control. (**c**) U373 cells were γ-irradiated with 10 Gy or treated with 5 μM etoposide and cells lysed at the indicated time points. MerTK expression was analysed by western blotting. (**d**) U373 cells expressing empty vector, MerTK-wt or MerTK-mut were treated with DMSO or 50 μM etoposide for 20 h. Half of the cells were lysed and analysed by western blotting with antibodies against total MerTK, P-MerTK, cleaved PARP and cleaved caspase-3. (**e**) The second half of the cells from **d** were analysed by flow cytometry for depolarization of mitochondrial membrane potential using JC-1: M1 apoptotic cells, M2 viable cells. A representative histogram is shown. The results were from three independently quantified experiments; data show mean ± s.d. The differences between MerTK-wt and empty vector or MerTK-mut expressing cells are significant ($P = 0.001$).

cells, respectively, but only a 20% increase in MerTK-wt-expressing cells (Figure 7e), demonstrating that MerTK kinase activity is crucial for its antiapoptotic function.

DISCUSSION

Current standard GBM therapy is restricted to tumour resection and subsequent radio/chemotherapy. In the clinic, the majority of patients with primary GBM experience disease recurrence within a few months because of the high infiltrative capacity of residual GBM cells.[2] Although the mechanism is still elusive, radioresistance and enhanced invasive potential of glioma cells after radiotherapy have been reported.[4,30,31] In addition, MerTK and Axl have recently been implicated in chemoresistance of astrocytoma cells.[28] In our study, we demonstrate that MerTK is upregulated and phosphorylated upon DNA damage, further addressing MerTK activity in glioma cell survival and invasion after ionizing radiation therapy.

GBM-derived spheres show highly heterogeneous features as primary tumours, including extensive infiltration *in vivo* and resistance to traditional therapies.[4,23] *In vitro* analyses of spheres maintained in suspension, as well as adherent and semi-adherent spheres showed no differences in proliferation rate.[24] However, the latter displayed either reduced tumour size or a well-delineated tumour border *in vivo*, whereas the suspended spheres always formed infiltrative tumours.[24] Interestingly, we found that MerTK is strongly suppressed in adherent/semi-adherent GBM-7S cells (Figure 3a). Knockdown of MerTK significantly interfered with cell invasion (Figure 4f) without affecting cell proliferation (data not shown). Invasion is initiated when tumour cells become detached from the growing tumour mass and invade into the surrounding parenchyma.[32] Cells lacking MerTK expression or activity showed elevated adherent capacity (Figures 3c, 4c and 5b),

possibly reflecting the involvement of MerTK activity in the establishment of signalling networks between tumour cells and the microenvironment *in vivo* and, thus, in an early step of tumour cell dissemination.[33-35]

Our data show that MerTK expression and phosphorylation in U373 cells is substantially upregulated during culture in NBM (Figures 4a and 5a). However, we did not detect Gas6 expression under both culture conditions (data not shown), suggesting the existence of undefined ligand(s) or mechanism(s) for MerTK activation. Our results reveals that inactivation of MerTK by mutating all three autophosphorylation sites hampers MerTK pro-invasive and antiapoptotic activities (Figures 5e and 7e), indicating that its kinase activity is crucial for MerTK involvement. Notably, overexpression of inactive MerTK in U373 cells severely decreased cell infiltration capacity (Figure 5e), possibly because of its competitive binding to signalling transducer(s), thus negatively influenced cell invasion.

Amoeboid-mesenchymal and mesenchymal-amoeboid transitions are dynamic processes and the actual transition of tumour cells is strongly influenced by the extracellular environment.[36] Conversion between two different migration patterns is commonly observed in cancer cells, including glioma cells.[6,36] The force leading to penetration of amoeboidly migrating cells through the extracellular matrix is sustained by cortical actomyosin contractility, which results in plasma membrane blebbing.[37] As we found that MerTK was required for the maintenance of rounded cell morphology and invasive capacity, it was hypothesized that MerTK positively regulates blebbing-associated mesenchymal-amoeboid transitions. Amoeboid migration depends largely on myosin activity regulated by the RhoA-ROCK signalling pathway via activation of MLC2.[38] Recently, MerTK was shown to promote glioma cell migration through regulating RhoA expression and FAK activity.[39] Our data demonstrate that knockdown of MerTK significantly attenuates the level of total MLC2 and P-MLC2 Ser19 (Figures 6a and b). Unlike U373 cells with a rounded amoeboid morphology under stem cell culture conditions, BS125, BS149 and U87MG cells survived but displayed elongated mesenchymal patterns (Supplementary Figure 4a). We did not detect upregulation of MerTK in such cells cultured in NBM (data not shown), suggesting that these GBM cell lines may not be amoeboidly mobile. MerTK was reported to regulate myosin II distribution during retinal pigment epithelial phagocytosis through association with the heavy chain of myosin IIA.[34] U373 cells expressing MerTK not only showed increased P-MLC2 Ser19 but were also more resistant to blebbistatin treatment (Figures 6a and d, Supplementary Figures 5a and b). These data suggest that MerTK may promote cell invasion by the regulation of myosin II activity.

Mesenchymally migrating cancer cells secrete matrix metalloproteinases, which facilitate metastasis or invasion.[40] Although invasive glioma cells migrate *in vitro* by degrading the pericellular matrix, *in vivo* studies suggest that matrix metalloproteinase-dependent proteolysis does not have a significant role in gliomas.[6] Clinical trials of matrix metalloproteinase inhibitors did not reveal evident benefits in the case of GBM or other cancer types.[41] Previous studies have demonstrated that cancer cells are able to invade in 3D after treatment with a matrix metalloproteinase inhibitor cocktail, whilst showing the typical features of amoeboid invasiveness during migration; this indicates that blocking extracellular matrix proteolysis promotes mesenchymal-amoeboid transitions.[36,42] Inhibition of the ATPase activity of actin and myosin could reduce cell motility,[43] but targeting such fundamental cytoskeleton components might have severe side effects. A further attractive therapeutic strategy for GBM treatment has been shown to target cell surface growth factor receptors such as epidermal growth factor receptor, platelet-derived growth factor receptor and vascular endothelial growth factor receptor. However, probably because of the unique biology of each glioblastoma and the redundant nature of signalling pathways, the overall clinical outcome has proven unsatisfactory.[2] Our results demonstrate that MerTK is not expressed in normal brain, and DNA damage-induced/activated MerTK not only promotes GBM cell survival, but also engages in tumour cell invasion. Therefore, combinatory targeting MerTK together with other 'switches' of signalling pathways may be of future therapeutic value in GBM treatment.

MATERIALS AND METHODS

Patients

Tissue samples of primary GBM were processed as described previously[44] in accordance with the guidelines of the Ethical Committee of the University Hospital of Basel and the University Hospital of Düsseldorf. Tumours were diagnosed and graded according to the World Health Organization classification of tumours of the nervous system.[45]

Construction of plasmids

The inactive MerTK autophosphorylation mutant MerTKY749FY753FY754F (MerTK-mut)[10] was generated by site-directed mutagenesis according to the manufacturer's instructions (Stratagene, La Jolla, CA, USA). Short hairpin RNA pairs 5′-GATCCCGGATGAACTGTATGAAATATTCAAGAGATATTTCATACAGTTCATCC TTTTTGGAAA-3′ and 5′-AGCTTTTCCAAAAAGGATGAACTGTATGAAATA TCTCTTGAATATTTCATACAGTTCATCCGG-3′ (targeting sequence was underlined) targeting human MerTK were inserted into the pSuper.retro.puro vector and pSuper.retro.puro-shLuc was used as a control.[46]

Cell culture and retroviral infection

Human GBM cell lines BS125, BS149, LN229, LN319 and U373 were cultured in Dulbecco's modified Eagle medium (DMEM) supplemented with 10% foetal bovine serum (FBS) (the 'BS' series was generated at the University of Basel, whereas the 'LN' series was the gift of Erwin Van Meir in Lausanne, Switzerland[47]). The GBM-derived spheres GBM-7S was previously characterized.[48] GBM-21S and GBM-22S were from University Hospitals and University of Geneva (Supplementary Table 1). These spheres were maintained in serum-free NeuralBasal Medium (Invitrogen, Carlsbad, CA, USA) supplemented with B27 (Invitrogen), N2 (Invitrogen), antibiotics (Invitrogen) and Glutamax (Invitrogen), plus 20 ng/ml EGF and 20 ng/ml bFGF from Peprotech (Rocky Hill, NJ, USA). U373 GBM cells transfected with pcDNA3.1(−) (vector), pcDNA3.1(−)-MerTK (MerTK-wt) or pcDNA3.1(−)-MerTK-mut (MerTK-mut) were selected in the presence of 1 mg/ml G418 (Gibco, North Andover, MA, USA). To produce recombinant retrovirus, 10 μg of DNA was transfected into 5×10^6 packaging cells in a 10-cm dish. After 24 h, the medium was replaced and incubated further at 32 °C for 48 h. For GBM-7S sphere infection, the cells were washed with phosphate-buffered saline to fully remove FBS and refreshed with NBM. To infect targeting cells, the supernatant containing recombinant retroviruses was filtered (0.45 μm, Millipore, Billerica, MA, USA) and incubated with the cells for 24 h in DMEM or NBM at 37 °C. Infected U373 cells and GBM-7S spheres were selected in the presence of 1 and 4 μg/ml of puromycin (Invitrogen), respectively. MerTK-depleted U373 cells transfected with pcDNA3-MerTK resistant cDNA were selected in the presence of 1 mg/ml G418 and 1 μg/ml of puromycin.

Antibodies

MerCT was raised against the C-terminus of human MerTK (amino acids 856–999). Antisera were purified by affinity purification and characterized by western blotting, IP and immunohistochemistry (Supplementary Figures 1a–c). The anti-MerTK mouse monoclonal antibodies 15R and 49S were raised against human MerTK (amino acids 536–999) and characterized by ELISA and western blotting (Supplementary Figure 1d). MerTK mouse monoclonal antibody CVO-311 was from Caveo Therapeutics, Inc. (Aurora, CO, USA), MerTK rabbit monoclonal Y323 from Abcam (Cambridge, MA, USA) and P-MerTK antibody from FabGennix Inc. (Frisco, TX, USA). P-MLC2

Ser19 and cleaved Caspase-3 antibodies were from Cell Signaling (Beverly, MA, USA), cleaved PARP antibody from BD Transduction Laboratories (San Jose, CA, USA), GFAP and total MLC2 antibodies (MY21) from Sigma (St Louis, MO, USA), and Nestin and actin antibodies from Santa Cruz (Santa Cruz, CA, USA). Alexa Fluor 647 phalloidin, goat anti-rabbit Alexa 488, goat anti-mouse Alexa 568 and goat anti-rabbit Alexa 647 were from Invitrogen and the Sox2 antibody from R&D Systems (Abingdon, Oxon, UK).

Immunofluorescence microscopy

Cells were processed for immunofluorescence as described previously.[49] To avoid morphological disruption by centrifugation, GBM spheres were precipitated by gravity. The medium was aspirated and the spheres were fixed with 4% PFA for 30 min and then permeabilized and blocked in 0.3% Triton X-100, 2% FBS and 1% bovine serum albumin for 1 h. Incubation with primary antibodies was performed overnight at 4 °C, followed by incubation with the secondary antibody for 1 h. DNA was counterstained with 4′-6-diamidino-2-phenylindole in VECTASHIELD mounting medium (Vectorlabs, Burlingame, CA, USA). Photographic images were obtained with a Zeiss Z1 wide-field microscope (Carl Zeiss AG, Oberkochen, Germany) and processed in Photoshop 6.0 (Adobe Systems Inc., San Jose, CA, USA).

Immunohistochemistry

Staining was performed with an automated instrument-reagent system (Discovery XT, Ventana Medical Systems Inc., Tucson, AZ, USA). Haematoxylin-counterstained sections were photographed (Nikon, Egg/ZH, Switzerland, YTHM) and analysed using ImageAccess Enterprise7 software (Glattbrugg, Switzerland).

Immunoblotting and IP

Protein extracts from tissues and cells were homogenized in immunoprecipitation buffer (20 mM Tris, 150 mM NaCl, 10% glycerol, 1% Triton X-100, 5 mM EDTA, 0.5 mM EGTA, 20 mM β-glycerophosphate, 50 mM NaF, 1 mM Na3VO4, 1 mM benzamidine, 4 μM leupeptin, 0.5 mM phenylmethylsulfonyl fluoride, 1 μM microcystine and 1 mM dithiothreitol at pH 8.0) and subjected to western blotting. For IP, the supernatant was incubated with anti-MerTK antibody MerCT overnight and incubated subsequently with protein A-sepharose (GE Healthcare, Zürich, Switzerland) for 3 h at 4 °C before the beads were washed four times in IP buffer and analysed by SDS–PAGE.

Quantitative real-time PCR analysis

Reverse transcriptase–PCR reactions on DNAase-treated RNA were performed using 2X SYBR Green mix (Applied Biosystems, Carlsbad, CA, USA) and an ABI Prism 7000 sequence detection system (Applied Biosystems). Relative expression of MerTK was normalized to the amount of eukaryotic translation elongation factor 1 alpha 1, a transcript that showed little variation in our microarray data.[21] MerTK was detected using forward and reverse primers 5′-ACTTCAGCCACCCAAATGTC-3′ and 5′-GGGC AATATCCACCATGAAC-3′.

Cell detachment assay

Dissociated GBM-7S spheres expressing shLuc or shMerTK were seeded in triplicate onto 12-well plates (0.3×10^6 per well) and incubated for 2 h. For U373 stable cell lines, cells were trypsinized and washed with phosphate-buffered saline to fully remove foetal bovine serum. Cells were then seeded in triplicate onto six-well plates (0.8×10^6 per well) in NBM and cultured for 48 h. The adherent and suspended cells were sorted and counted with Vi-Cell (Beckman Coulter, Nyon, Switzerland).

3D cultures

Growth factor reduced-Matrigel (GFR-Matrigel, BD Biosciences, Basel, Switzerland; 100 μl) was pipetted into BD Falcon8-well CultureSlides. Single-cell suspensions (~500 cells in 100 μl NBM) were loaded into each well. After 24 h, a further 200 μl of NBM was added and replaced every 2–3 days.

γ-irradiation treatments

Cells were plated at consistent densities 24 h before treatment. Following a single-dose γ-irradiation treatment in a TORREX 120D (Astrophysics Research Corp., City of Industry, CA, USA) instrument at 5 mA/120 kV and 0.13 Gy/s, cells were left to recover at 37 °C for the indicated times before analysis.

Invasion assay

The invasive capacity of U373 cells expressing empty vector, MerTK-wt, or MerTK-mut and U373 cells infected with pSuper-retro carrying control or MerTK shRNA were evaluated by Boyden Chamber Assay (BD BioCoat Tumour Invasion Assay System, BD Biosciences) with minor modifications. Briefly, 5×10^4 serum-starved cells were seeded into the upper chamber and the bottom wells filled with NBM. After a 22-h incubation, cells that had invaded the Matrigel matrix membrane were counterstained with 4′-6-diamidino-2-phenylindole. The number of invading cells was counted under a fluorescent microscope.

Apoptosis measurement

Cells undergoing apoptosis were harvested, washed with phosphate-buffered saline and subdivided into two fractions. One fraction was stained with JC-1 (5,5′,6,6′-tetrachloro-1,1′,3,3′-tetraethylbenzimidazolylcarbocyanine iodide, Molecular Probes, Invitrogen) and subjected to flow cytometry for detection of mitochondrial depolarization ($\Delta\psi m$). Red fluorescence (FL-2 channel) of JC-1 (J-aggregates) indicated intact mitochondria, whereas green fluorescence (FL-1 channel) showed monomeric JC-1 produced by the breakdown of $\Delta\psi m$ during apoptosis. The remaining cells were lysed for western blotting.

CONFLICT OF INTEREST

Virginie Clément-Schatlo (VCS) is co-inventor and co-author of four patents filed by the University of Geneva and Geneva University Hospitals. VCS is co-founder and shareholder of Stemergie Biotechnology, SA. VCS is part-time employee as Chief Scientific Officer at Stemergie Biotechnology, SA. The other authors declare no conflict of interest.

ACKNOWLEDGEMENTS

We thank Sandrine Bichet and Hubertus Kohler for helping with immunohistochemistry and FACS experiments, respectively, Susanne Schenk for the generation of the MerTK monoclonal antibody, Douglass Vollrath for the pcDNA3.1(−)-MerTK construct, Janis Liebetanz and Doriano Fabbro for the GST-hMerTK (amino acids 536–999) construct and Patrick King for editing the manuscript. This research was funded by Oncosuisse CCRP Grant KFP OCS-01613-12-2004. G Xue is supported by the Swiss National Science Foundation SNF 31003A_130838. The FMI is part of the Novartis Research Foundation.

REFERENCES

1 Furnari FB, Fenton T, Bachoo RM, Mukasa A, Stommel JM, Stegh A *et al.* Malignant astrocytic glioma: genetics, biology, and paths to treatment. *Genes Dev* 2007; **21**: 2683–2710.
2 Van Meir EG, Hadjipanayis CG, Norden AD, Shu HK, Wen PY, Olson JJ. Exciting new advances in neuro-oncology: the avenue to a cure for malignant glioma. *CA Cancer J Clin* 2010; **60**: 166–193.
3 Zhai GG, Malhotra R, Delaney M, Latham D, Nestler U, Zhang M *et al.* Radiation enhances the invasive potential of primary glioblastoma cells via activation of the Rho signaling pathway. *J Neurooncol* 2006; **76**: 227–237.
4 Bao S, Wu Q, McLendon RE, Hao Y, Shi Q, Hjelmeland AB *et al.* Glioma stem cells promote radioresistance by preferential activation of the DNA damage response. *Nature* 2006; **444**: 756–760.
5 Bellail AC, Hunter SB, Brat DJ, Tan C, Van Meir EG. Microregional extracellular matrix heterogeneity in brain modulates glioma cell invasion. *Int J Biochem Cell Biol* 2004; **36**: 1046–1069.
6 Beadle C, Assanah MC, Monzo P, Vallee R, Rosenfeld SS, Canoll P. The role of myosin II in glioma invasion of the brain. *Mol Biol Cell* 2008; **19**: 3357–3368.

7 Graham DK, Dawson TL, Mullaney DL, Snodgrass HR, Earp HS. Cloning and mRNA expression analysis of a novel human protooncogene, c-mer. *Cell Growth Differ* 1994; **5**: 647 - 657.
8 Linger RM, Keating AK, Earp HS, Graham DK. TAM receptor tyrosine kinases: biologic functions, signaling, and potential therapeutic targeting in human cancer. *Adv Cancer Res* 2008; **100**: 35 - 83.
9 Nagata K, Ohashi K, Nakano T, Arita H, Zong C, Hanafusa H *et al.* Identification of the product of growth arrest-specific gene 6 as a common ligand for Axl, Sky, and Mer receptor tyrosine kinases. *J Biol Chem* 1996; **271**: 30022 - 30027.
10 Ling L, Templeton D, Kung HJ. Identification of the major autophosphorylation sites of Nyk/Mer, an NCAM-related receptor tyrosine kinase. *J Biol Chem* 1996; **271**: 18355 - 18362.
11 Duncan JL, Yang H, Vollrath D, Yasumura D, Matthes MT, Trautmann N *et al.* Inherited retinal dystrophy in Mer knockout mice. *Adv Exp Med Biol* 2003; **533**: 165 - 172.
12 Cohen PL, Caricchio R, Abraham V, Camenisch TD, Jennette JC, Roubey RA *et al.* Delayed apoptotic cell clearance and lupus-like autoimmunity in mice lacking the c-mer membrane tyrosine kinase. *J Exp Med* 2002; **196**: 135 - 140.
13 Hafizi S, Dahlback B. Signalling and functional diversity within the Axl subfamily of receptor tyrosine kinases. *Cytokine Growth Factor Rev* 2006; **17**: 295 - 304.
14 Ling L, Kung HJ. Mitogenic signals and transforming potential of Nyk, a newly identified neural cell adhesion molecule-related receptor tyrosine kinase. *Mol Cell Biol* 1995; **15**: 6582 - 6592.
15 Ek S, Hogerkorp CM, Dictor M, Ehinger M, Borrebaeck CA. Mantle cell lymphomas express a distinct genetic signature affecting lymphocyte trafficking and growth regulation as compared with subpopulations of normal human B cells. *Cancer Res* 2002; **62**: 4398 - 4405.
16 Wu YM, Robinson DR, Kung HJ. Signal pathways in up-regulation of chemokines by tyrosine kinase MER/NYK in prostate cancer cells. *Cancer Res* 2004; **64**: 7311 - 7320.
17 Tavazoie SF, Alarcon C, Oskarsson T, Padua D, Wang Q, Bos PD *et al.* Endogenous human microRNAs that suppress breast cancer metastasis. *Nature* 2008; **451**: 147 - 152.
18 Gyorffy B, Lage H. A Web-based data warehouse on gene expression in human malignant melanoma. *J Invest Dermatol* 2007; **127**: 394 - 399.
19 Graham DK, Salzberg DB, Kurtzberg J, Sather S, Matsushima GK, Keating AK *et al.* Ectopic expression of the proto-oncogene Mer in pediatric T-cell acute lymphoblastic leukemia. *Clin Cancer Res* 2006; **12**: 2662 - 2669.
20 Verhaak RG, Hoadley KA, Purdom E, Wang V, Qi Y, Wilkerson MD *et al.* Integrated genomic analysis identifies clinically relevant subtypes of glioblastoma characterized by abnormalities in PDGFRA, IDH1, EGFR, and NF1. *Cancer Cell* 2010; **17**: 98 - 110.
21 Grzmil M, Morin Jr P, Lino MM, Merlo A, Frank S, Wang Y *et al.* MAP kinase-interacting kinase 1 regulates SMAD2-dependent TGF-beta signaling pathway in human glioblastoma. *Cancer Res* 2011; **71**: 2392 - 2402.
22 Sather S, Kenyon KD, Lefkowitz JB, Liang X, Varnum BC, Henson PM *et al.* A soluble form of the Mer receptor tyrosine kinase inhibits macrophage clearance of apoptotic cells and platelet aggregation. *Blood* 2007; **109**: 1026 - 1033.
23 Lee J, Kotliarova S, Kotliarov Y, Li A, Su Q, Donin NM *et al.* Tumor stem cells derived from glioblastomas cultured in bFGF and EGF more closely mirror the phenotype and genotype of primary tumors than do serum-cultured cell lines. *Cancer Cell* 2006; **9**: 391 - 403.
24 Gunther HS, Schmidt NO, Phillips HS, Kemming D, Kharbanda S, Soriano R *et al.* Glioblastoma-derived stem cell-enriched cultures form distinct subgroups according to molecular and phenotypic criteria. *Oncogene* 2008; **27**: 2897 - 2909.
25 Ropolo M, Daga A, Griffero F, Foresta M, Casartelli G, Zunino A *et al.* Comparative analysis of DNA repair in stem and nonstem glioma cell cultures. *Mol Cancer Res* 2009; **7**: 383 - 392.
26 Pankova K, Rosel D, Novotny M, Brabek J. The molecular mechanisms of transition between mesenchymal and amoeboid invasiveness in tumor cells. *Cell Mol Life Sci* 2010; **67**: 63 - 71.
27 Zhang M, Rao PV. Blebbistatin, a novel inhibitor of myosin II ATPase activity, increases aqueous humor outflow facility in perfused enucleated porcine eyes. *Invest Ophthalmol Vis Sci* 2005; **46**: 4130 - 4138.
28 Keating AK, Kim GK, Jones AE, Donson AM, Ware K, Mulcahy JM *et al.* Inhibition of Mer and Axl receptor tyrosine kinases in astrocytoma cells leads to increased apoptosis and improved chemosensitivity. *Mol Cancer Ther* 2010; **9**: 1298 - 1307.
29 Vichalkovski A, Gresko E, Cornils H, Hergovich A, Schmitz D, Hemmings BA. NDR kinase is activated by RASSF1A/MST1 in response to Fas receptor stimulation and promotes apoptosis. *Curr Biol* 2008; **18**: 1889 - 1895.
30 Hambardzumyan D, Squatrito M, Holland EC. Radiation resistance and stem-like cells in brain tumors. *Cancer Cell* 2006; **10**: 454 - 456.
31 McCord AM, Jamal M, Williams ES, Camphausen K, Tofilon PJ. CD133+ glioblastoma stem-like cells are radiosensitive with a defective DNA damage response compared with established cell lines. *Clin Cancer Res* 2009; **15**: 5145 - 5153.
32 Nakada M, Nakada S, Demuth T, Tran NL, Hoelzinger DB, Berens ME. Molecular targets of glioma invasion. *Cell Mol Life Sci* 2007; **64**: 458 - 478.
33 Wu Y, Singh S, Georgescu MM, Birge RB. A role for Mer tyrosine kinase in alphavbeta5 integrin-mediated phagocytosis of apoptotic cells. *J Cell Sci* 2005; **118**: 539 - 553.
34 Strick DJ, Feng W, Vollrath D. Mertk drives myosin II redistribution during retinal pigment epithelial phagocytosis. *Invest Ophthalmol Vis Sci* 2009; **50**: 2427 - 2435.
35 Guttridge KL, Luft JC, Dawson TL, Kozlowska E, Mahajan NP, Varnum B *et al.* Mer receptor tyrosine kinase signaling: prevention of apoptosis and alteration of cytoskeletal architecture without stimulation or proliferation. *J Biol Chem* 2002; **277**: 24057 - 24066.
36 Wolf K, Mazo I, Leung H, Engelke K, von Andrian UH, Deryugina EI *et al.* Compensation mechanism in tumor cell migration: mesenchymal-amoeboid transition after blocking of pericellular proteolysis. *J Cell Biol* 2003; **160**: 267 - 277.
37 Fackler OT, Grosse R. Cell motility through plasma membrane blebbing. *J Cell Biol* 2008; **181**: 879 - 884.
38 Parri M, Chiarugi P. Rac and Rho GTPases in cancer cell motility control. *Cell Commun Signal* 2010; **8**: 23.
39 Rogers AE, Le JP, Sather S, Pernu BM, Graham DK, Pierce AM *et al.* Mer receptor tyrosine kinase inhibition impedes glioblastoma multiforme migration and alters cellular morphology. *Oncogene* 2011; doi:10.1038/onc.2011.588.
40 Cukierman E, Pankov R, Yamada KM. Cell interactions with three-dimensional matrices. *Curr Opin Cell Biol* 2002; **14**: 633 - 639.
41 Coussens LM, Fingleton B, Matrisian LM. Matrix metalloproteinase inhibitors and cancer: trials and tribulations. *Science* 2002; **295**: 2387 - 2392.
42 Wyckoff JB, Pinner SE, Gschmeissner S, Condeelis JS, Sahai E. ROCK- and myosin-dependent matrix deformation enables protease-independent tumor-cell invasion *in vivo*. *Curr Biol* 2006; **16**: 1515 - 1523.
43 Rao J, Li N. Microfilament actin remodeling as a potential target for cancer drug development. *Curr Cancer Drug Targets* 2004; **4**: 345 - 354.
44 Maier D, Comparone D, Taylor E, Zhang Z, Gratzl O, Van Meir EG *et al.* New deletion in low-grade oligodendroglioma at the glioblastoma suppressor locus on chromosome 10q25-26. *Oncogene* 1997; **15**: 997 - 1000.
45 Louis DN, Ohgaki H, Wiestler OD, Cavenee WK, Burger PC, Jouvet A *et al.* The 2007 WHO classification of tumours of the central nervous system. *Acta Neuropathol* 2007; **114**: 97 - 109.
46 Hergovich A, Lamla S, Nigg EA, Hemmings BA. Centrosome-associated NDR kinase regulates centrosome duplication. *Mol Cell* 2007; **25**: 625 - 634.
47 Ishii N, Maier D, Merlo A, Tada M, Sawamura Y, Diserens AC *et al.* Frequent co-alterations of TP53, p16/CDKN2A, p14ARF, PTEN tumor suppressor genes in human glioma cell lines. *Brain Pathol* 1999; **9**: 469 - 479.
48 Clement V, Marino D, Cudalbu C, Hamou MF, Mlynarik V, de Tribolet N *et al.* Marker-independent identification of glioma-initiating cells. *Nat Methods* 2010; **7**: 224 - 228.
49 Hergovich A, Lisztwan J, Barry R, Ballschmieter P, Krek W. Regulation of microtubule stability by the von Hippel-Lindau tumour suppressor protein pVHL. *Nat Cell Biol* 2003; **5**: 64 - 70.

Supplementary Information accompanies the paper on the Oncogene website (http://www.nature.com/onc)